Heliyon 10 (2024) e38712

Contents lists available at ScienceDirect

Heliyon

journal homepage: www.cell.com/heliyon

Research article

Unveiling the Mysteries of the Chinese lens zonule balance tension: A statistical analysis

Lujie Zhang [a,b,1], Kai Wen [a,1], Ming Liu [a,1], Jie Wang [a], Yifang Huang [a], Yufeng Zhang [a], Ruihua Wei [a,**], Jing Sun [a,*]

[a] Tianjin Key Laboratory of Retinal Functions and Diseases, Tianjin Branch of National Clinical Research Center for Ocular Disease, Eye Institute and School of Optometry, Tianjin Medical University Eye Hospital, China
[b] Tianjin Children's Hospital, Tianjin Key Laboratory of Birth Defects for Prevention and Treatment, China

ARTICLE INFO

Keywords:
Lens zonules balance tension
Lens gravity
Lens volume

ABSTRACT

Background: This study aims to provide an estimated dataset of lens zonule balance tension (LZBT) measurements in cataractous lenses among Chinese patients and to conduct a statistical analysis of anterior segment parameters.
Methods: This is a cross-sectional study. We included a total of 833 eyes from 833 Chinese participants aged 23–91 years who underwent cataract surgery. Anterior segment parameters were measured using swept-source anterior segment optical coherence tomography (SS-AS OCT) to calculate lens gravity (LG) and crystalline lens volume (VOL). Axial length (AL) was measured using IOL-Master 700. LZBT was calculated using force decomposition and synthesis methods.
Results: The mean LZBT in the horizontal direction was 8.48E-05 ± 3.23E-05 N across all eyes. The LZBT in the subtemporal-supraspinal and supraspinal-temporal directions was $\sqrt{2}$ times greater than in the vertical direction. The balanced force on the suspensory ligament in the horizontal direction was twice as strong as in the vertical direction. Additionally, anterior segment parameters such as lens equivalent diameter (LE-dia), radius of the anterior lens surface curvature (RAL), radius of the posterior lens surface curvature (RPL), anterior chamber depth (ACD), iris area, iris volume, and iris thickness showed positive correlations with AL.
Conclusions: Accounting for gravitational effects, we concluded that zonule force is asymmetrically distributed. Importantly, this study establishes the normal range of LZBT across different meridians using force synthesis and decomposition, offering new insights and feasibility for studying suspensory ligament biomechanics.

1. Background

Lens zonules, also known as the suspensory ligament of the lens, are a complex system of extracellular fibers that center the lens in the eye [1]. Naturally, the zonules remain hidden from view as they are located just behind the iris. The less one understands their importance, the more crucial they become in medical practice, particularly for ophthalmologists. The integrity of the zonules

* Corresponding author. No. 251, Fukang Road, Nankai District, Tianjin, 300110, China .
** Corresponding author. No. 251, Fukang Road, Nankai District, Tianjin, 300110, China.
E-mail addresses: weirhua2009@126.com (R. Wei), TMUeye@163.com (J. Sun).
[1] They are both first authors, contributed equally.

https://doi.org/10.1016/j.heliyon.2024.e38712
Received 10 July 2024; Received in revised form 27 September 2024; Accepted 27 September 2024
Available online 30 September 2024

significantly influences whether cataract surgeries will be "uneventful" or "challenging." Weakened suspensory ligaments may rupture due to changes in intraoperative pressure or the effects of the surgeon's operating force, causing considerable complications for ophthalmologists. In addition, suspensory ligament abnormalities can lead to inaccurate intraocular lens (IOL) results by affecting the accuracy of the effective lens position and resulting in unstable postoperative vision. A weakened suspensory ligament can also cause dislocation of the IOL after cataract surgery, which can severely impair a patient's visual function. Therefore, understanding the condition of the zonules prior to surgery is critical for avoiding surgical complications and minimizing intraoperative and postoperative risks [2].

The zonular apparatus consists of three groups of fibers that span the space between the equatorial edge of the lens and the tip of the ciliary body, working together to maintain the lens's position and function. Obvious signs of lens zonule abnormalities include lens tremor, subluxation or a shallow anterior chamber. However, these symptoms can be subtle and easily overlooked in clinical practice. Ultrasound biomicroscopy is necessary for patients with suspected suspension ligament relaxation or dissociation. Unfortunately, lens zonules are not easily accessible for many patients, making clear examination and accurate evaluation of their functional status an ongoing challenge for ophthalmologists. Multiple finite element analyses have been used to evaluate zonular forces, utilizing in vitro data for simulations [3,4]. However, no method currently exists for evaluating lens zonule tension (LZT) using direct patient measurement parameters.

The CASIA 2 (Tomey Corp.), the latest swept-source anterior segment optical coherence tomography (SS-AS OCT), offers higher resolution and deeper scanning depth (13 mm). It is widely used in clinics due to its ease of use, speed of acquisition, and non-contact design [5]. CASIA 2 can automatically and accurately measure lens equivalent diameter (LE-dia), lens thickness (LT), lens vault (LV), and optical density (LOD) through its built-in software. It also allows for analysis of anterior segment parameters, such as the lens volume (VOL) and radius of the anterior/posterior lens surface curvature [6,7].

In this study, we aimed to estimate the lens zonule balance tension (LZBT) in Chinese cataractous lenses by examining the differences in zonule tension across opposing directions on the same meridian. We studied the distribution and associated factors of LZBT to provide a reference for cataract surgery planning, estimating effective lens positions, and refining intraocular lens formulas. To achieve this, we conducted a comprehensive statistical analysis of anterior segment parameters across cohorts with varying axial lengths. We then assessed the correlations between these parameters and axial length. Using a subset of these anterior segment parameters, we mathematically estimated the LZBT, applying a scientific and methodological approach.

2. Methods

This single-center, cross-sectional, in vivo study included 833 eyes from patients who underwent cataract surgery at Tianjin Medical University Eye Hospital (Tianjin, China) between March 2022 and February 2023. Participants were randomly selected, and the following exclusion criteria were applied: (1) ocular diseases affecting the anterior structures, including glaucoma, uveitis, lens subluxation, and aniridia; (2) a history of ocular surgery, laser treatment, or trauma; (3) corneal abnormalities affecting imaging, such as leukoma, keratoconus, or corneal scarring; and (4) poor fixation leading to low image quality or inability to cooperate during the examinations. All participants underwent imaging with the IOL-Master 700 (Carl Zeiss Meditec AG) and CASIA 2 devices. The study adhered to the tenets of the Declaration of Helsinki and was approved by the Ethics Committee of Tianjin Medical University Eye Hospital. Written informed consent was obtained from all the participants.

2.1. Anterior segment parameter measurements

All subjects underwent CASIA 2 imaging with natural pupils using the 16-scan lens biometry mode while seated. In recent years, the emergence of CASIA 2 (Tomey Corporation, Nagoya, Japan), representing the second generation of anterior segment optical coherence tomography (OCT), has revolutionized the field. This advanced system integrates Fourier domain technology with frequency-swept source OCT technology, enabling significant enhancements in scanning capabilities. Specifically, it boasts an expedited scanning speed of 50 000 A-scans per second, an extended scanning depth reaching 16 × 16 × 13 mm, an intensified scanning density, and a heightened imaging resolution, thereby advancing the precision and efficacy of anterior segment assessment in a scholarly context. The lens equatorial plane was automatically captured using the built-in CASIA 2 software, which extended the anterior and posterior lens surfaces to intersect at the lenticular periphery. The values of LT, LD, LOD, LV, tilt, decentration (descent), RAL, and RPL were automatically generated in 3D by CASIA 2. Anterior chamber depth (ACD) was also measured. Axial length (AL) was measured using the IOL-Master 700. LT and LE-dia were used to calculate VOL and lens gravity (LG).

2.2. Calculation of LG

The VOL was calculated from the LT and LE-dia, assuming the VOL is approximately the sum of two different semi-ellipsoids as follows [7,8]:

$$VOL = \frac{\pi}{6} \times LT^2 \times LE\text{—}dia$$

LOD is the absorption coefficient of the lens per unit distance at a given wavelength λ. We used the LOD as the density of the lens to calculate its mass. LG was calculated from the VOL and LOD as follows:

$$LG = LM(\text{lens mass}) \times g = VOL \times LOD \times g$$

2.3. Calculation of LZBT

In the vertical direction, three forces act on the lens to maintain its neutrality: the force of the upper lens zonules (FUZ), the force of the lower lens zonules (FLZ), and LG. The relationship is described as:

$$FUZ = FLZ + LG$$

Therefore, the LZBTv in the vertical direction is:

$$LZBTv = FUZ - FLZ = LG \tag{1}$$

By decomposing the vertical force, we calculated the LZT in the subnasal (FLNZ)–supratemporal (FSTZ) and subtemporal (FLTZ)–supratemporal (FSNZ) directions (OS). According to Pythagorean's theorem, the LZT in the subnasal-supratemporal direction is as follows:

$$sin\ 45^\circ \times (FLZ + LG) + FLNZ = sin\ 45^\circ \times FUZ + FSTZ$$

$$FLNZ - FSTZ = sin\ 45^\circ \times (FLZ + LG) - sin\ 45^\circ \times FUZ$$

$$FLNZ - FSTZ = \frac{\sqrt{2}}{2}(FLZ + LG - FUZ) = \sqrt{2}LG$$

$$LZBT(LN, ST) = FLNZ - FSTZ = \sqrt{2}LG$$

Similarly, the LZT in the subtemporal-supranasal direction is calculated as follows:

$$LZBT(LT, SN) = FLTZ - FSNZ = \sqrt{2}LG \tag{2}$$

In the horizontal direction, the balance of the LZT is:

$$\begin{aligned} FNZ - FTZ = {} & sin\ 45^\circ \left(FLTZ + sin\ 45^\circ (FLZ + LG)\right) + sin\ 45^\circ (FSTZ + sin\ 45^\circ FUZ) \\ & - sin\ 45^\circ \left(FLNZ \right. \\ & \left. + sin\ 45^\circ (FLZ + LG)\right) - sin\ 45^\circ (FSNZ + sin\ 45^\circ FUZ) \\ = {} & \frac{\sqrt{2}}{2}\left(FLTZ + \frac{\sqrt{2}}{2}(FLZ + LG)\right) + \frac{\sqrt{2}}{2}\left(FSTZ + \frac{\sqrt{2}}{2}FUZ\right) \\ & - \frac{\sqrt{2}}{2}\left(FLNZ + \frac{\sqrt{2}}{2}(FLZ + LG)\right) - \frac{\sqrt{2}}{2}(FSNZ + \frac{\sqrt{2}}{2}FUZ) \\ = {} & \frac{\sqrt{2}}{2}FLTZ + \frac{1}{2}(FLZ + LG) + \frac{\sqrt{2}}{2}FSTZ + \frac{1}{2}FUZ - \frac{\sqrt{2}}{2}FLNZ - \frac{1}{2}(FLZ + LG) \\ & - \frac{\sqrt{2}}{2}FSNZ - \frac{1}{2}FUZ = \frac{\sqrt{2}}{2}(FLTZ - FSNZ) + \frac{\sqrt{2}}{2}(FSTZ - FLNZ) = LG + LG = 2LG \end{aligned}$$

So

$$LZBTh = 2\ LG \tag{3}$$

The relationships between the LZT in all directions are shown in Fig. 1.

With reference to published articles [9,10], the participants were further divided into four AL groups (short eyes, AL<22 mm; normal eyes, AL 22–24.5; moderately myopic eyes, AL 24.5–26 mm; and highly myopic eyes, AL >26 mm).

3. Data analysis

Statistical analyses were performed using GraphPad Prism software (v. 10.1.1; GraphPad Software). Statistical significance was defined as $P < 0.05$. All continuous variables are expressed as mean ± SD. The Kolmogorov–−Smirnov test was used to assess data normality ($P > 0.05$). Depending on the data distribution, a one-way analysis of variance (ANOVA) was used to compare differences among the groups. Locally estimated scatterplot smoothing (LOESS) curves were generated to assess the distribution trends of VOL, LT, LD, RAL, and RPL with AL in the eyes with cataracts. Univariate regression models were created using the ordinary least squares (OLS) method to fit these trends, and the Akaike information criterion (AIC) was used to choose the best-fit models. Pearson's correlation analysis was performed to identify potential factors associated with lens dimensions, and multivariate linear regression models were

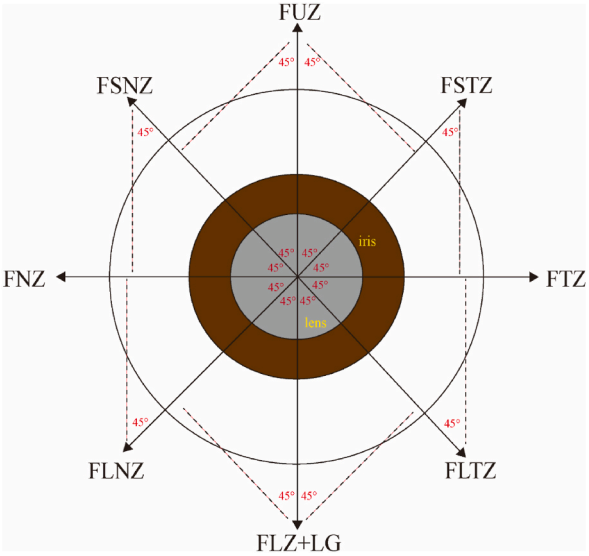

Fig. 1. Schematic diagram of the decomposition and synthesis of lens zonules under tension and gravity.

used to analyze the candidate determinants of VOL, lens mass (LM), and LG. The strength of the correlations was graded by the Pearson coefficient (r) as follows: negligible correlation (|r| = 0.00 to 0.10), weak correlation (|r| = 0.10 to 0.39), moderate correlation (|r| = 0.40 to 0.69), strong correlation (|r| = 0.70 to 0.89), and very strong correlation (|r| = 0.90 to 1.00).

4. Results

A total of 833 eyes from 833 833 Chinese cataract participants (age range: 23–91 years) were included. Baseline characteristics are

Table 1
Characteristics of the study participants and the distributions of eye parameters.

Variables	All eyes	Short eyes AL<22 mm	Normal eyes AL 22–24.5 mm	Moderately myopic eyes AL 24.5–26 mm	Highly myopic eyes AL >26 mm	P value
Participants/eyes (n)	833/833	49/49	573/573	96/96	115/115	
Age (y), mean ± SD (range)	68.88 ± 9.79 (23–91)	70.71 ± 7.71 (52–89)	70.91 ± 8.79 (26–91)	68.39 ± 11.70 (28–88)	65.64 ± 12.16 (23–87)	> 0.05
Sex (M), n (%)	346(41.54)	7(14.29)	236(41.19)	59(61.46)	44(38.26)	
Ocular biometry, mean ± SD						
AL (mm)	24.11 ± 2.04	21.60 ± 0.39	23.32 ± 0.61	25.07 ± 0.44	28.32 ± 1.99	<0.0001
LT (mm)	4.57 ± 0.49	4.68 ± 0.45	4.61 ± 0.48	4.40 ± 0.48	4.41 ± 0.55	< 0.0001
LE-dia (mm)	9.75 ± 1.06	9.46 ± 1.02	9.75 ± 1.06	9.75 ± 1.15	9.87 ± 1.01	0.1307
RAL (mm)	9.45 ± 1.39	8.27 ± 0.77	9.26 ± 1.13	10.32 ± 1.63	10.18 ± 1.78	< 0.0001
RPL (mm)	5.70 ± 1.16	5.38 ± 0.93	5.70 ± 1.10	5.74 ± 1.25	5.84 ± 1.38	0.1391
ACD (mm)	2.67 ± 0.46	2.27 ± 0.43	2.58 ± 0.41	2.97 ± 0.38	3.0 ± 0.43	< 0.0001
LOD	39.50 ± 8.52	38.27 ± 8.09	39.23 ± 8.21	38.97 ± 9.23	39.79 ± 9.62	0.6437
LV (mm)	0.19 ± 0.39	0.32 ± 0.70	0.25 ± 0.34	0.03 ± 0.29	−0.01 ± 0.35	<0.0001
Tilt (°)	5.01 ± 1.75	5.74 ± 1.66	5.13 ± 1.62	4.82 ± 2.13	4.23 ± 1.86	< 0.0001
Decent(mm)	0.18 ± 0.12	0.19 ± 0.11	0.17 ± 0.12	0.19 ± 0.12	0.18 ± 0.10	0.2754
Iris area(mm2)	1.42 ± 0.24	1.33 ± 0.19	1.41 ± 0.24	1.50 ± 0.26	1.43 ± 0.22	< 0.0001
Iris volume(mm3)	32.50 ± 4.99	29.47 ± 4.86	32.08 ± 4.76	35.16 ± 5.17	33.58 ± 4.91	0.0006
Iris thickness(mm)	21.58 ± 10.99	19.21 ± 7.42	21.66 ± 12.54	21.49 ± 6.43	22.23 ± 5.67	< 0.0001
VOL (mm^3)	108.8 ± 31.00	110.4 ± 28.58	111.00 ± 31.11	101.20 ± 29.68	103.20 ± 31.16	0.0052
LG(N)	4.24E-05 ± 1.61E-05	4.21E-05 ± 1.60E-05	4.34E-05 ± 1.59E-05	3.91E-05 ± 1.56E-05	4.09e-05 ± 1.69e-05	0.0675
LM (kg)	4.34E-06 ± 1.64E-06	4.30E-06 ± 1.63E-06	4.44E-06 ± 1.62E-06	3.99E-06 ± 1.60E-06	4.17E-06 ± 1.73 E−06	> 0.05

presented in Table 1.

4.1. Distributions of anterior segment parameters and impact of AL

The mean LODs were 38.27 ± 8.09 for short eyes, 39.23 ± 8.21 for normal eyes, 38.97 ± 9.23 for moderately myopic eyes, and 39.79 ± 9.62 for highly myopic eyes (Table 1, Supplementary Fig. 1). There was no significant difference in LOD across different ALs (Supplementary Figs. 1B and $P > 0.05$). The mean VOL was 110.4 ± 28.58 mm^3 in short eyes, 111.00 ± 31.11 mm^3 in normal eyes, 101.20 ± 29.68 mm^3 in moderately myopic eyes, and 103.20 ± 31.16 mm^3 in highly myopic eyes (Table 1, Supplementary Fig. 1). ANOVA revealed that the distribution of VOLs with ALs decreased (VOL = −1.265 × AL+140.2 mm3) ($P < 0.05$, Supplementary Fig. 1C). Pearson's analysis indicated that VOL was positively correlated with age, LT, LE-dia, RPL, LV, VOL, and LM, and negatively correlated with AL, RAL, ACD, iris area, and iris volume (Table 2). According to multivariate linear regression analysis, there were correlations between VOLs and age, LT, LE-dia, LOD, and lens descent ($P < 0.001$; Table 3). The mean values for the LG were 4.21E-05 ± 1.60E-05 N in short eyes, 4.34E-05 ± 1.59E-05 N in normal eyes, 3.91E-05 ± 1.56E-05 N in moderately myopic eyes, and 4.09E-05 ± 1.69E-05 N in highly myopic eyes (Table 1). Similar to the difference in LOD, there was no significant difference in LG length between patients with different ALs (Supplementary Fig. 1E). Pearson's analysis revealed that LG was positively correlated with age, LT, LE-dia, RPL, LV, VOL, and LM and negatively correlated with RAL and ACD, iris area and iris volume (Table 2). Multivariate linear regression showed correlations between LG and age, LT, LE-dia, and VOL ($P < 0.001$; Table 3).

Notably, anterior segment parameters, including LE-dia, RAL, RPL, ACD, iris area, iris volume, and iris thickness, were positively correlated with AL and negatively correlated with the eye axes, including LT, LV, title, and VOL (Supplementary Figs. 2A–H, Fig. 3A–H, and Fig. 4A–F).

4.2. Distribution of LZBTs in patients with cataract

Our results showed that LZBT in the subtemporal-supraspinal-temporal and supraspinal-temporal direction was $\sqrt{2}$ times greater than in the vertical direction (Formula 2, Table 4). The balanced force of the suspensory ligament in the horizontal direction was twice as strong as that in the vertical direction (Formula 3, Table 4). Normal values for LZBT in the horizontal and vertical directions were (8.26E −005,8.70E-005) and (4.14E-05,4.35E −05), respectively, while the normal values for the oblique axis were (5.84E-05,6.15E-05).

5. Discussion

This study, involving 833 Chinese cataract participants, presented a dataset of LTBZs across a wide age range, including patients with short, normal, moderately myopic, and highly myopic eyes. It revealed no significant correlation between LTBZ and AL in cataractous eyes.

Owing to the technical limitations of inspection equipment and the concealment of anatomical locations, assessing the state of the lens zonules has long been a technical challenge for ophthalmologists. Historically, ophthalmologists have relied mainly on the AL to roughly judge the state of the lens capsule and zonules in patients with cataracts. However, this method has significant drawbacks. For example, a long AL, large capsular bag, and weakened suspensory ligaments do not always correlate perfectly [11]. Establishing normal ranges for VOL and LT provides a reference point for identifying patients with larger capsular bags after phacoemulsification [7]. However, this method cannot directly evaluate the condition of the lens zonules. Therefore, establishing a normal reference range for LTBZ levels is vital. In this study, we used force decomposition and synthesis to estimate the normal range of LTBZ across four meridians (Fig. 1), providing a new approach to studying the state of the suspensory ligament.

For the calculation of the VOL, we followed methods recognized by the academic community [7,8]. Interestingly, the VOL values we calculated were relatively small compared to previous research [7,12–14]. In addition, we discovered that patients with longer ALs tend to have smaller VOLs. Further analysis of LE-dia and LT revealed that while LE-dia increased in patients with long ALs, the LT decreased. The key point is that the LT accounts for a larger proportion of the VOL calculation. This finding also indicates that the lens shape in patients with cataract with longer ALs is flatter. Our other results confirmed this: as the AL increased, RAL increased, while LV decreased (Table 1, Supplementary Fig. 2E, Fig. 2G and 3G). However, multiple linear regression analysis revealed no correlation between VOLs and ALs but revealed strong correlations with age, LT, LE-dia, LOD, and lens descent.

Lens tilt and decentration were also investigated. The results showed that the longer the AL, the smaller the tilt (Supplementary Fig. 3C). However, no correlation was observed between decentration and AL (Supplementary Fig. 3E). This finding suggests that flat lenses are less likely to tilt. These findings align with previous research [15–17]. We also found that iris volume positively correlated with AL (Table 1, Supplementary Fig. 4E). If we consider the structure of the anterior segment as a whole, it is possible that there is a balance between lens and iris volumes as the AL changes to adapt to the spatial constraints of the anterior segment. Patients with shorter ALs exhibited greater lens tilt, possibly due to the greater compressive force exerted on the lens within the limited space of the anterior segment.

LOD is a complex characteristic that slows the speed of light propagation and produces a refractive effect. Previous studies have shown that CASIA 2 demonstrated good consistency with Pentacam in the measurement of lens density and that it provides a reliable alternative densitometric measurement method [6,18]. This consistency was one of the main reasons we used LOD to calculate the lens quality. Our results indicated no correlation between LOD and AL (Table 1, Supplementary Fig. 1A), possibly because we did not

Table 2
Correlations between VOL, LG, LM, and potential determinants by Pearson analysis.

Variables	Determinants	All eyes		Short eyes AL<22		Normal eyes AL 22 to 24.5		Moderately myopic eyes AL 24.5 to 26		Highly myopic eyes AL >26 mm	
VOL (mm^3)		r	P value	r	P value	r	P value	r	P value	r	P value
	Age (y)	0.271	<0.0001	0.265	0.0657	0.250	<0.0001	0.218	0.0326	0.328	0.0004
	AL (mm)	−0.083	0.0168	0.034	0.8174	0.085	0.0424	0.240	0.0186	0.123	0.1893
	LT (mm)	0.934	<0.0001	0.923	<0.0001	0.935	<0.0001	0.924	<0.0001	0.954	<0.0001
	LE-dia (mm)	0.719	<0.0001	0.797	<0.0001	0.726	<0.0001	0.737	<0.0001	0.730	<0.0001
	RAL (mm)	−0.251	<0.0001	−0.069	0.6483	−0.207	<0.0001	−0.258	0.0125	−0.340	0.0003
	RPL (mm)	0.388	<0.0001	0.536	<0.0001	0.421	<0.0001	0.512	<0.0001	0.1956	0.0362
	ACD (mm)	−0.567	<0.0001	−0.672	<0.0001	−0.580	<0.0001	−0.561	<0.0001	−0.569	<0.0001
	LV (mm)	0.526	<0.0001	0.414	0.0034	0.534	<0.0001	0.549	<0.0001	0.6345	<0.0001
	Iris area(mm^2)	−0.083	0.0166	0.122	0.4041	−0.072	0.0837	−0.152	0.1382	−0.054	0.5679
	Iris volume(mm^3)	−0.105	0.0036	−0.080	0.6108	−0.090	0.0375	−0.049	0.6480	−0.045	0.6456
	Iris thickness(mm)	−0.039	0.2613	0.058	0.6918	−0.033	0.4245	−0.079	0.4437	−0.115	0.2227
	Tilt (°)	−0.094	0.0064	0.050	0.7333	−0.154	0.0002	−0.109	0.2925	−0.022	0.8136
	Decent(mm)	−0.022	0.5228	0.0693	0.6362	0.021	0.6119	0.063	0.5441	−0.097	0.3023
LG(N)	Age (y)	0.274	<0.0001	0.247	0.0875	0.251	<0.0001	0.248	0.0149	0.351	<0.0001
	AL (mm)	−0.043	0.2122	0.027	0.8563	−0.101	0.0152	0.173	0.0910	0.188	0.0438
	LT (mm)	0.790	<0.0001	0.806	<0.0001	0.794	<0.0001	0.778	<0.0001	0.793	<0.0001
	LE-dia (mm)	0.548	<0.0001	0.628	<0.0001	0.544	<0.0001	0.530	<0.0001	0.593	<0.0001
	RAL (mm)	−0.146	0.0002	−0.011	0.9419	−0.133	0.0017	−0.099	0.3445	−0.175	0.0673
	RPL (mm)	0.2725	<0.0001	0.3489	0.0151	0.312	<0.0001	0.275	0.0067	0.135	0.1519
	ACD (mm)	−0.471	<0.0001	−0.657	<0.0001	−0.504	<0.0001	−0.415	<0.0001	−0.419	<0.0001
	LV (mm)	0.438	<0.0001	0.3720	0.0092	0.468	<0.0001	0.405	<0.0001	0.446	<0.0001
	LOD	0.676	<0.0001	0.780	<0.0001	0.662	<0.0001	0.717	<0.0001	0.687	<0.0001
	VOL (mm^3)	0.809	<0.0001	0.8450	<0.0001	0.804	<0.0001	0.786	<0.0001	0.825	<0.0001
	LM (kg)	0.995	<0.0001	1.000	<0.0001	0.993	<0.0001	1.000	<0.0001	1.000	<0.0001
	Iris area(mm^2)	−0.079	0.0232	−0.044	0.7621	−0.064	0.1250	−0.174	0.0894	−0.018	0.8479
	Iris volume(mm^3)	−0.098	0.0064	−0.154	0.3249	−0.079	0.0669	−0.117	0.2733	−0.020	0.8333
	Iris thickness(mm)	−0.000	0.9888	0.041	0.7786	0.012	0.7758	−0.116	0.2609	−0.050	0.5958
	Tilt (°)	−0.038	0.2772	−0.019	0.8982	−0.088	0.0360	−0.013	0.9012	0.060	0.5239
	Decent(mm)	−0.034	0.3205	−0.093	0.5246	−0.021	0.6140	0.103	0.3195	−0.170	0.0701
LM (kg)	Age (y)	0.274	<0.0001	0.247	0.0875	0.251	<0.0001	0.248	0.0149	0.351	<0.0001
	AL (mm)	−0.044	0.2076	0.027	0.8563	−0.093	0.0263	0.173	0.0912	0.188	0.0443
	LT (mm)	0.795	<0.0001	0.806	<0.0001	0.801	<0.0001	0.778	<0.0001	0.793	<0.0001
	LE-dia (mm)	0.554	<0.0001	0.628	<0.0001	0.554	<0.0001	0.530	<0.0001	0.593	<0.0001
	RAL (mm)	−0.145	0.0002	−0.011	0.9419	−0.129	0.0022	−0.010	0.3438	−0.175	0.0682
	RPL (mm)	0.284	<0.0001	0.349	0.0151	0.330	<0.0001	0.275	0.0067	0.135	0.1510
	ACD (mm)	−0.477	<0.0001	−0.657	<0.0001	−0.513	<0.0001	−0.415	<0.0001	−0.419	<0.0001
	LV (mm)	0.441	<0.0001	0.372	0.0092	0.472	<0.0001	0.405	<0.0001	0.446	<0.0001
	LOD	0.678	<0.0001	0.780	<0.0001	0.664	<0.0001	0.717	<0.0001	0.687	<0.0001
	VOL (mm^3)	0.815	<0.0001	0.845	<0.0001	0.814	<0.0001	0.786	<0.0001	0.825	<0.0001
	LG(N)	0.995	<0.0001	1.000	<0.0001	0.993	<0.0001	1.000	<0.0001	1.000	<0.0001
	Iris area(mm^2)	−0.084	0.0159	−0.044	0.7621	−0.071	0.0890	−0.174	0.0895	−0.018	0.8508
	Iris volume(mm^3)	−0.098	0.0065	−0.154	0.3249	−0.079	0.0693	−0.117	0.2731	−0.020	0.8369
	Iris thickness(mm)	−0.007	0.8337	0.041	0.7786	0.003	0.9404	−0.116	0.2182	−0.050	0.5958
	Tilt (°)	−0.043	0.2193	−0.019	0.8982	−0.096	0.0212	−0.013	0.2604	0.060	0.5248
	Decent(mm)	−0.039	0.2578	−0.093	0.5246	−0.027	0.5120	0.103	0.3198	−0.169	0.0705
Tilt	Age (y)	0.111	0.0013	0.180	0.2164	0.015	0.7240	0.209	0.0409	0.139	0.1385
	AL (mm)	−0.195	<0.0001	−0.088	0.5473	−0.090	0.0324	−0.149	0.1473	0.059	0.5320
	LT (mm)	−0.019	0.5886	0.097	0.5089	−0.090	0.0304	−0.081	0.4328	0.055	0.5619

(*continued on next page*)

Table 2 (*continued*)

Variables	Determinants	All eyes		Short eyes AL<22		Normal eyes AL 22 to 24.5		Moderately myopic eyes AL 24.5 to 26		Highly myopic eyes AL >26 mm	
	LE-dia (mm)	−0.197	<0.0001	−0.062	0.6681	−0.211	<0.0001	−0.117	0.2572	−0.211	0.0234
	RAL (mm)	−0.090	0.0100	−0.289	0.0512	0.017	0.6946	0.012	0.9125	−0.139	0.1472
	RPL (mm)	−0.154	<0.0001	0.016	0.9133	−0.170	<0.0001	−0.186	0.0698	−0.056	0.5491
	ACD (mm)	−0.103	0.0029	−0.065	0.6597	−0.016	0.6858	0.071	0.4934	−0.107	0.2561
	LV (mm)	0.042	0.2280	0.097	0.5128	−0.030	0.4757	−0.248	0.0148	0.169	0.0719
	LOD	0.049	0.1607	−0.082	0.5755	0.029	0.4933	0.117	0.2567	0.134	0.1528
	VOL (mm^3)	−0.094	0.0064	0.050	0.7333	−0.154	0.0002	−0.109	0.2925	−0.022	0.8136
	LG(N)	−0.038	0.2772	−0.019	0.8982	−0.088	0.0360	−0.013	0.9012	0.060	0.5239
	LM (kg)	−0.043	0.2193	−0.019	0.8982	−0.096	0.0212	−0.013	0.9015	0.060	0.5248
	Iris area(mm^2)	0.024	0.4968	0.088	0.5471	0.030	0.4728	0.061	0.5544	0.063	0.5056
	Iris volume(mm^3)	−0.040	0.2665	0.078	0.6212	0.007	0.8761	0.009	0.0016	−0.017	0.8594
	Iris thickness(mm)	−0.044	0.2033	0.111	0.4490	−0.006	0.8789	−0.318	0.0010	−0.125	0.1824
	Decent(mm)	0.164	<0.0001	0.385	0.0062	0.217	<0.0001	0.116	0.2621	−0.072	0.4438
Decent	Age (y)	0.040	0.2456	0.324	0.0231	0.050	0.2344	0.138	0.1802	−0.108	0.2494
	AL (mm)	0.033	0.3453	0.102	0.4845	0.027	0.5123	−0.037	0.7220	−0.001	0.9884
	LT (mm)	−0.020	0.5738	0.028	0.8507	−0.017	0.6922	0.086	0.4035	−0.089	0.3464
	LE-dia (mm)	−0.077	0.0257	0.090	0.5396	−0.088	0.0360	−0.060	0.5596	−0.104	0.2685
	RAL (mm)	−0.006	0.8614	−0.118	0.4343	−0.070	0.1002	0.027	0.7958	0.161	0.0934
	RPL (mm)	−0.051	0.1400	0.050	0.7365	−0.051	0.2229	−0.116	0.2616	−0.029	0.7584
	ACD (mm)	−0.001	0.9845	−0.018	0.9023	−0.042	0.3145	0.018	0.8585	0.1098	0.2427
	LV (mm)	−0.049	0.1589	−0.315	0.0291	0.006	0.8950	−0.021	0.8370	−0.058	0.5366
	LOD	0.001	0.9783	−0.209	0.1496	0.013	0.7596	0.192	0.0608	−0.142	0.1306
	VOL (mm^3)	−0.022	0.5228	0.069	0.6362	−0.021	0.6119	0.063	0.5441	−0.097	0.3023
	LG(N)	−0.034	0.3205	−0.093	0.5246	−0.021	0.6140	0.103	0.3195	−0.170	0.0701
	LM (kg)	−0.039	0.2578	−0.093	0.5246	−0.027	0.5120	0.103	0.3198	−0.169	0.0705
	Iris area(mm^2)	0.033	0.3438	−0.026	0.8615	0.049	0.2401	0.049	0.6367	−0.073	0.4394
	Iris volume(mm^3)	0.022	0.5402	−0.084	0.5914	0.029	0.5052	−0.001	0.9955	0.011	0.9075
	Iris thickness(mm)	−0.094	0.0066	−0.182	0.2104	−0.094	0.0249	−0.176	0.0866	0.025	0.8087
	Tilt (°)	0.164	<0.0001	0.385	0.0062	0.217	<0.0001	0.116	0.2621	−0.072	0.7874

Table 3
Multivariate linear regression analysis of the relationships between VOL, LG, LM and potential determinants.

	Variables	All eyes (n = 833) (adj R2 = 0.9805)			
VOL (mm^3)		β	95 % CI	Standardized β	P value
	Age (y)	−0.07199	−0.1078, −0.03616	0.01825	<0.0001
	AL (mm)	0.04138	−0.1338, 0.2166	0.08923	0.6430
	LT (mm)	49.47	48.47, 50.47	0.5103	<0.0001
	LE-dia (mm)	10.28	9.825, 10.74	0.2331	<0.0001
	RAL (mm)	0.02412	−0.2713, 0.3195	0.1505	0.8727
	RPL (mm)	0.3550	−0.007839, 0.7179	0.1848	0.0551
	ACD (mm)	1.334	0.02526, 2.642	0.6664	0.0457
	LV (mm)	0.9132	−0.5494, 2.376	0.7450	0.2207
	LOD	−0.06190	−0.1004, 0.02338	0.01962	0.0017
	Tilt (°)	−0.1325	−0.3260, 0.06094	0.09854	0.1791
	Decent(mm)	6.688	3.733, 9.643	1.505	<0.0001
	Variables	All eyes (n = 833) (adj R2 = 0.9626)			
LG (N)		β	95 % CI	Standardized β	P value
	Age (y)	−4.558e-008	−7.123e-008, -1.994e-008	1.306e-008	<0.0001
	AL (mm)	−3.215e-010	−1.257e-007, 1.250e-007	6.384e-008	0.9960
	LT (mm)	1.832e-005	1.760e-005, 1.904e-005	3.651e-007	<0.0001
	LE-dia (mm)	3.959e-006	3.631e-006, 4.287e-006	1.670e-007	<0.0001
	RAL (mm)	1.004e-007	−1.112e-007, 3.121e-007	1.078e-007	0.3518
	RPL (mm)	1.863e-007	−7.327e-008, 4.459e-007	1.322e-007	0.1592
	ACD (mm)	−3.861e-007	−1.323e-006, 5.505e-007	4.771e-007	0.4186
	LV (mm)	−9.855e-008	−1.146e-006, 9.485e-007	5.334e-007	0.8535
	LOD	1.037e-006	1.010e-006, 1.065e-006	1.405e-008	<0.0001
	Tilt (°)	1.717e-008	−1.212e-007, 1.556e-007	7.050e-008	0.8076
	Decent(mm)	−1.704e-006	−3.819e-006, 4.107e-007	1.077e-006	0.1141
		All eyes (n = 833) (adj R2 = 0.9627)			
LM (kg)		β	95 % CI	Standardized β	P value
	Age (y)	−4.693e-009	−7.309e-009, -2.077e-009	1.333e-009	<0.0001
	AL (mm)	−1.358e-010	−1.293e-008, 1.265e-008	6.515e-009	0.9834
	LT (mm)	1.870e-006	1.797e-006, 1.943e-006	3.726e-008	<0.0001
	LE-dia (mm)	4.049e-007	3.715e-007, 4.383e-007	1.702e-008	<0.0001
	RAL (mm)	1.093e-008	−1.064e-008, 3.250e-008	1.099e-008	0.3201
	RPL (mm)	1.896e-008	−7.527e-009, 4.546e-008	1.349e-008	0.1603
	ACD (mm)	−4.140e-008	−1.369e-007, 5.412e-008	4.865e-008	0.3951
	LV (mm)	−1.236e-008	−1.191e-007, 9.442e-008	5.439e-008	0.8203
	LOD	1.059e-007	1.031e-007, 1.087e-007	1.433e-009	<0.0001
	Tilt (°)	1.850e-009	−1.227e-008, 1.597e-008	7.194e-009	0.7971
	Decent(mm)	−1.775e-007	−3.933e-007, 3.824e-008	1.099e-007	0.1067
		All eyes (n = 833) (adj R2 = 0.1324)			
Tilt (°)		β	95 % CI	Standardized β	P value
	Age (y)	0.007241	−0.006418, 0.02090	0.006957	0.2983
	AL (mm)	−0.1293	−0.1945, −0.06405	0.03321	0.0001
	LT (mm)	0.6959	−0.7083, 2.100	0.7153	0.3309
	LE-dia (mm)	−0.1516	−0.4820, 0.1788	0.1683	0.3680
	RAL (mm)	0.01371	−0.09722, 0.1246	0.05651	0.8083
	RPL (mm)	−0.01818	−0.1547, 0.1184	0.06954	0.7939
	ACD (mm)	−0.4906	−0.9826, 0.001344	0.2506	0.0506
	LV (mm)	−0.0004016	−0.5515, 0.5507	0.2807	0.8203
	LOD	−0.009785	−0.05564, 0.03607	0.02336	0.6754
	VOL (mm3)	1.850e-009	−0.05302, 0.005856	0.01500	0.1162
	Decent(mm)	2.596	1.475, 3.717	0.5711	<0.0001
		All eyes (n = 833) (adj R2 = 0.0726)			
Decent (mm)		β	95 % CI	Standardized β	P value
	Age (y)	0.0006455	−0.0002289, 0.001520	0.0004454	0.1477
	AL (mm)	0.005878	0.001662, 0.01009	0.002147	0.0063
	LT (mm)	−0.1870	−0.2759, −0.09806	0.04530	<0.0001
	LE-dia (mm)	−0.04988	−0.07070, −0.02905	0.01061	<0.0001
	RAL (mm)	3.686e-005	−0.007107, 0.007180	0.003639	0.9919
	RPL (mm)	0.002421	−0.006374, 0.01122	0.004480	0.5890
	ACD (mm)	−0.02440	−0.05608, 0.007270	0.01613	0.1308
	LV (mm)	−0.01706	−0.05244, 0.01833	0.01802	0.3443
	LOD	0.0002009	−0.0007369, 0.001139	0.0004777	0.6742
	VOL (mm3)	0.003911	0.002183, 0.005639	0.0008802	<0.0001
	Tilt (°)	0.01059	0.005965, 0.01521	0.002354	<0.0001

Table 4
The LZBT in all directions.

Variables	All eyes	Short eyes AL<22	Normal eyes AL 22 to 24.5	Moderately myopic eyes AL 24.5 to 26	Highly myopic eyes AL >26 mm
Participants/eyes (n)	833/833	49/49	573/573	96/96	115/115
Age (y), Mean ± SD (range)	68.88 ± 9.79 (23–91)	70.71 ± 7.71 (52–89)	70.91 ± 8.79 (26–91)	68.39 ± 11.70 (28–88)	65.64 ± 12.16 (23–87)
Sex (M), n (%)	346(41.54)	7(14.29)	236(41.19)	59(61.46)	44(38.26)
LZBTv(N)	4.24E-05 ± 1.61E-05 95 % CI (4.14E-05,4.35E −05)	4.22E-05 ± 1.60E-05	4.34E-05 ± 1.59E-05	3.91E-05 ± 1.56E-05	4.09E-05 ± 1.69E-05
LZBT(LN,ST)	5.60E-05 ± 2.28E-05 95 % CI (5.84E-05,6.15E-05)	5.96E-05 ± 2.26E-05	6.13E-05 ± 2.26E-05	5.51E-05 ± 2.22E-05	5.79E-05 ± 2.40E-05
LZBT(LT,SN)	5.60E-05 ± 2.28E-05 95 % CI (5.84E-05,6.15E-05)	5.96E-05 ± 2.26E-05	6.13E-05 ± 2.26E-05	5.51E-05 ± 2.22E-05	5.79E-05 ± 2.40E-05
LZBTh	8.48E-05 ± 3.23E-005 95 % CI (8.26E −05,8.70E-05)	8.43E-005 ± 3.20E-05	8.66E-05 ± 3.20E-05	7.80E-05 ± 3.14E-05	8.18E-05 ± 3.40E-05

classify cataracts using the Lens Opacities Classification System III.

LG was calculated based on LOD and VOL ($LG = VOL \times LOD \times g$). One study reported that gravity can affect lens position, providing evidence of the ability of zonules to slacken during strong accommodation [19]. However, some researchers have questioned the reliability of these findings [20,21]. Nevertheless, we believe that gravity does affect the suspensory ligaments of the lens. We defined the force on the lens as a node of 45° at 4 meridians–0-180°, 45°–225°, 90°–270°, and 135°–315°. LTBZ was defined as the force in the direction opposite to the zonule force on the same meridian. Considering the gravitational force on the lens, we calculated that LTBZ in the vertical direction was equal to LG. As the meridian changed in the horizontal direction, the LTBZ gradually increased and reached its maximum value (twice the gravitational force) along the 0–180° axis (Table 4). This indicates that while the lens remained neutral, the zonule forces were asymmetrically distributed.

Most importantly, this study is the first to determine LTBZ in different directions (Table 4). Compared to other indirect evaluation indicators commonly used in clinical practice, such as AL, LTBZ is undoubtedly more direct and accurate in evaluating the status of the suspensory ligament. This will enable a clearer prediction of the degree of suspensory ligament relaxation before cataract surgery. Furthermore, our findings have two significant implications. First, they constitute a valuable reference for pre-operative planning in cataract surgery. Specifically, an LTBZ that exceeds our calculated normal range may suggest potential zonular laxity in the patient, necessitating heightened surgeon awareness and the implementation of preemptive strategies. Second, deviations in lens equilibrium force from the norm can compromise the accuracy of the estimated effective lens position, thereby influencing the precision of the targeted refractive outcome. Consequently, for these patients, it is imperative to provide a thorough pre-operative explanation and clarification to ensure informed decision-making. In addition to not considering the horizontal decomposition of suspensory ligament forces, the study has other limitations. It focused solely on a Chinese population, which may limit the generalizability of the findings to other ethnicities. Additionally, the study did not classify cataracts using the Lens Opacities Classification System III, which could have influenced the correlation between lens opacity density (LOD) and axial length (AL). Lastly, the cross-sectional nature of the study prevents assessment of longitudinal changes in lens zonule tension (LTBZ) and its impact over time, limiting insights into the progression of zonular weakening.

In conclusion, we generated a comprehensive dataset of LTBZ, VOL, and LG across a wide age range of patients with cataract in a Chinese population. Through an analysis of AL, LT, LE-dia, LV, RAL, and RPL, we found that the shape of the lens in patients with cataract with long ALs was flattened. Considering the effect of gravity, we concluded that the zonule force was not symmetrically distributed. Most importantly, this study established the normal range of suspensory ligament balance forces across different meridians using force synthesis and decomposition, offering a novel and feasible approach for studying suspensory ligaments. These findings provide a new basis for evaluating suspensory ligament status before cataract surgery. Future studies could explore the generalizability of lens zonule tension (LTBZ) findings across diverse populations and investigate longitudinal changes in LTBZ to assess the progression of zonular weakening. Additionally, integrating advanced imaging techniques and incorporating cataract classification systems could enhance accuracy in evaluating lens and suspensory ligament conditions preoperatively.

Ethics approval and consent to participate

This study was approved by the Human Research Ethics Committee of Tianjin Medical University Eye Hospital and adhered to the tenets of the Helsinki Declaration of 1975, as revised in 2000 (5). Informed consent was obtained from all patients included in the study.

Funding

This work was supported by the [Sponsored by Tianjin Binhai New Area Health Research Project ,China (Grant No.2023BWKQ019 and NO.2023BWKZ007); Tianjin Medical University Eye Hospital High-level Innovative Talent Programme ,China (Grant No. YDYYRCXM-E2023-04)].

Availability of data and materials

The datasets generated during and analyzed during the current study are not publicly available because we are conducting further research but are available from the corresponding author upon reasonable request.

CRediT authorship contribution statement

Lujie Zhang: Writing – original draft, Data curation. **Kai Wen:** Writing – original draft, Methodology, Investigation, Formal analysis, Data curation. **Ming Liu:** Data curation. **Jie Wang:** Data curation. **Yifang Huang:** Data curation. **Yufeng Zhang:** Data curation. **Ruihua Wei:** Writing – review & editing, Validation, Supervision. **Jing Sun:** Writing – review & editing, Validation, Supervision, Methodology.

Declaration of competing interest

The authors declare that they have no known competing financial interests or personal relationships that could have appeared to influence the work reported in this paper.

Appendix A. Supplementary data

Supplementary data to this article can be found online at https://doi.org/10.1016/j.heliyon.2024.e38712.

References

[1] S. Bassnett, Zinn's zonule, Prog. Retin. Eye Res. 82 (2021) 100902.
[2] Y. Pan, Z. Liu, H. Zhang, Research progress of lens zonules, Adv Ophthalmol Pract Res 3 (2023) 80–85.
[3] K.R. Knaus, A. Hipsley, S.S. Blemker, The action of ciliary muscle contraction on accommodation of the lens explored with a 3D model, Biomech. Model. Mechanobiol. 20 (2021) 879–894.
[4] R.A. Schachar, et al., Finite element analysis of zonular forces, Exp. Eye Res. 237 (2023) 109709.
[5] J.F. Bille, C.H. Cham (Eds.), High Resolution Imaging in Microscopy and Ophthalmology: New Frontiers in Biomedical Optics, 2019.
[6] W. Wang, et al., Objective quantification of lens nuclear opacities using swept-source anterior segment optical coherence tomography, Br. J. Ophthalmol. 106 (2022) 790–794.
[7] K. Chen, et al., Distribution and associated factors of crystalline lens volume in noncataract adolescents and adults and patients with cataract in a Chinese population, J. Cataract Refract. Surg. 49 (2023) 783–789.
[8] M. Modesti, G. Pasqualitto, R. Appolloni, I. Pecorella, P. Sourdille, Preoperative and postoperative size and movements of the lens capsular bag: ultrasound biomicroscopy analysis, J. Cataract Refract. Surg. 37 (2011) 1775–1784.
[9] J.X. Kane, A. Van Heerden, A. Atik, C. Petsoglou, Accuracy of 3 new methods for intraocular lens power selection, J. Cataract Refract. Surg. 43 (2017) 333–339.
[10] X. Rong, et al., Intraocular lens power calculation in eyes with extreme myopia: comparison of Barrett Universal II, Haigis, and Olsen formulas, J. Cataract Refract. Surg. 45 (2019) 732–737.
[11] B.C. Giers, R. Khoramnia, L.F. Weber, T. Tandogan, G.U. Auffarth, Rotation and decentration of an undersized plate-haptic trifocal toric intraocular lens in an eye with moderate myopia, J. Cataract Refract. Surg. 42 (2016) 489–493.
[12] G.O.t. Waring, D.H. Chang, K.M. Rocha, L. Gouvea, R. Penatti, Correlation of intraoperative optical coherence tomography of crystalline lens diameter, thickness, and volume with biometry and age, Am. J. Ophthalmol. 225 (2021) 147–156.
[13] E. Martinez-Enriquez, et al., Age-Related changes to the three-dimensional full shape of the isolated human crystalline lens, Invest. Ophthalmol. Vis. Sci. 61 (2020) 11.
[14] A. Mohamed, et al., Isolated human crystalline lens three-dimensional shape: a comparison between Indian and European populations, Exp. Eye Res. 205 (2021) 108481.
[15] Q. Lu, W. He, D. Qian, Y. Lu, X. Zhu, Measurement of crystalline lens tilt in high myopic eyes before cataract surgery using swept-source optical coherence tomography, Eye Vis (Lond) 7 (2020) 14.
[16] L. Wang, R. Guimaraes de Souza, M.P. Weikert, D.D. Koch, Evaluation of crystalline lens and intraocular lens tilt using a swept-source optical coherence tomography biometer, J. Cataract Refract. Surg. 45 (2019) 35–40.
[17] X. Chen, et al., Distributions of crystalline lens tilt and decentration and associated factors in age-related cataract, J. Cataract Refract. Surg. 47 (2021) 1296–1301.
[18] Y. Xu, et al., Comparison of corneal and lens density measurements obtained by Pentacam and CASIA2 in myopes, BMC Ophthalmol. 23 (2023) 448.
[19] L.J. Lister, M. Suheimat, P.K. Verkicharla, E.A. Mallen, D.A. Atchison, Influence of gravity on ocular lens position, Invest. Ophthalmol. Vis. Sci. 57 (2016) 1885–1891.
[20] R.A. Schachar, Gravity does not affect lens position during accommodation, Invest. Ophthalmol. Vis. Sci. 57 (2016) 4566–4567.
[21] D.A. Atchison, L.J. Lister, M. Suheimat, P.K. Verkicharla, E.A. Mallen, Author response: gravity affects lens position during accommodation, Invest. Ophthalmol. Vis. Sci. 57 (2016) 4568–4569.